Infiltration and Seepage through Fractured Welded Tuff

T. A. Ghezzehei[1], P. F. Dobson[1], J. A. Rodriguez[2], and P. J. Cook[1]

[1] *Earth Sciences Division, Lawrence Berkeley National Laboratory, Berkeley, California, USA*
[2] *Centro de Investigacion sobre Sequia, Instituto de Ecologia, Aldama, Chihuahua, Mexico*

Abstract─ *The Nopal I mine in Peña Blanca, Chihuahua, Mexico, contains a uranium ore deposit within fractured tuff. Previous mining activities exposed a level ground surface 8 m above an excavated mining adit. In this paper, we report results of ongoing research to understand and model percolation through the fractured tuff and seepage into a mined adit both of which are important processes for the performance of the proposed nuclear waste repository at Yucca Mountain. Travel of water plumes was modeled using one-dimensional numerical and analytical approaches. Most of the hydrologic property estimates were calculated from mean fracture apertures and fracture density. Based on the modeling results, we presented constraints for the arrival time and temporal pattern of seepage at the adit.*

I. INTRODUCTION

A uranium ore deposit at Nopal I (Peña Blanca, Chihuahua, Mexico) has been investigated extensively as a natural analogue for understanding unsaturated flow and radionuclide transport processes in the proposed nuclear waste repository at Yucca Mountain. Geologic similarity between Nopal I and Yucca Mountain in terms of rock type and fracturing provides a unique opportunity to test the conceptual and numerical models used for flow and transport modeling at Yucca Mountain.

Previous mining activities at the site exposed two horizontal surfaces (+10 and +00 levels) with a vertical separation of approximately 10 m. In addition, about 8 m below the +10 level, a mining adit approximately 2 m high was excavated (**Figure 1**). Rainwater collected at the +10 level percolates through the fractured rock and seeps into the adit. The goal of this study is to develop and test a flow and transport model of the Nopal I site by integrating hydrological, meteorological, and geological data. At present, seepage data at the adit is being collected.

The objective of this paper is to report results of preliminary models that provide constraints on the expected seepage response at Nopal I.

II. NUMERICAL MODELING

II.A. Model Development

Previous studies [1] have characterized the hydrologic properties of the matrix of the Nopal ash-flow tuff using cores (core diameter ranges from 1.9 cm to 7.6 cm) obtained from five rock samples collected at the

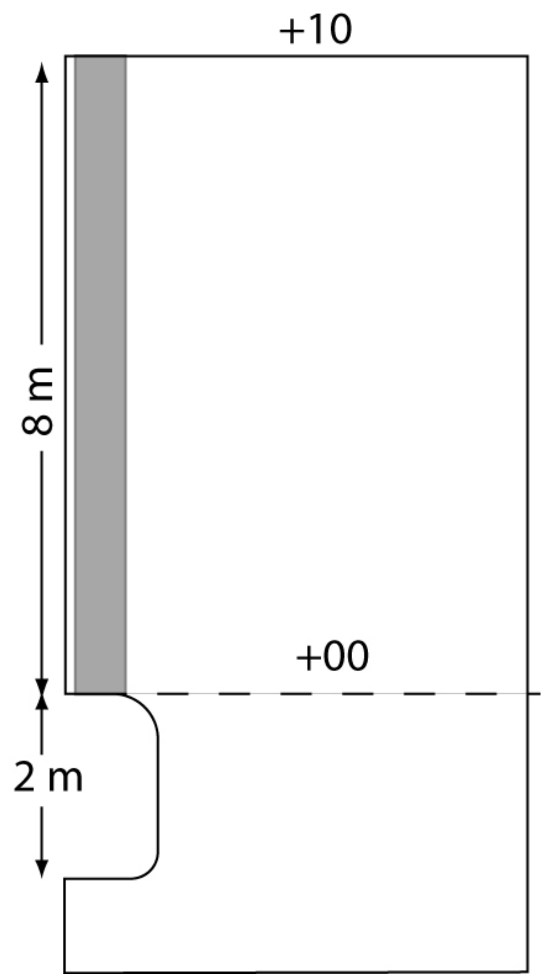

Figure 1. Schematic diagram showing the location of the adit 8 m below the excavated horizontal surface at +10 level (note that figure shows only half of the adit because of symmetry). The shaded region represents the one-dimensional model used to predict seepage.

+10 level. Porosity, permeability, and water retention curves of the cores were determined in a laboratory. Based on these samples, the matrix porosity (by gravimetric method) ranges from 0.078 to 0.255, and the corresponding saturated hydraulic conductivity ranges from 10^{-12} m/s to 9.5×10^{-10} m/s (0.03 mm/yr to 30mm/yr). Based on simulations that use these measured matrix properties and assumed fracture properties, *Green and Rice* [1] concluded that water introduced at the ground surface takes from a few days to 1,000 years to reach the adit.

Moreover, uranium transport studies [2] suggest that greater transport distances from the ore deposit were achieved along a few relatively continuous fractures with apertures wider than 1 mm and extending to more than 10 m. A detailed survey of the outcrop at +10 level indicated that the tuff at Nopal I is highly fractured, with most fractures being less than 1 m long and occurring as groups of subparallel breaks [2]. Therefore, the contribution of the matrix to percolation and seepage is not accounted for in this report.

In this preliminary assessment, the fractured tuff between the +10 level and the adit is conceptualized as one-dimensional (1D) columns (with cross sectional area of 1 m^2). The fracture network of each column is represented by a set of vertical fractures with mean aperture of b [L] and density of d [L^{-1}]. The permeability k [L^2] of the 1D columns is estimated using the *cubic law* [3, 4],

$$k = \frac{b^3\, d}{12} \tag{1}$$

This model overestimates permeability of fractures that have sharp irregularities [5, 6].

Similarly, the air-entry pressure of the mean fracture aperture (ψ_o [M L^{-1} T^{-2}]) is estimated using the *Laplace-Young* equation,

$$\psi_o = \frac{2\gamma}{b} \tag{2}$$

where γ [M T^{-2}] is the surface tension of water. The fracture porosity of the column is

$$\phi = b\, d \tag{3}$$

The capillary pressure and relative permeability of the fracture continuum are expressed using the *van Genuchten* [7] relations,

Table 1. Estimated hydrologic properties of the fracture continuum for different fracture apertures and densities

b [μm]	d [m^{-1}]	k [m^{-2}]	ψ_o [Pa]	ϕ	T_{min} [1] [hr]
10	1	$8.33\cdot10^{-17}$	14540	0.00001	27.2
10	10	$8.33\cdot10^{-16}$	14540	0.0001	27.2
10	100	$8.33\cdot10^{-15}$	14540	0.001	27.2
20	1	$6.67\cdot10^{-16}$	7270	0.00002	6.8
20	10	$6.67\cdot10^{-15}$	7270	0.0002	6.8
20	100	$6.67\cdot10^{-14}$	7270	0.002	6.8
50	1	$1.04\cdot10^{-14}$	2908	0.00005	1.1
50	10	$1.04\cdot10^{-13}$	2908	0.0005	1.1
50	100	$1.04\cdot10^{-12}$	2908	0.005	1.1
100	1	$8.33\cdot10^{-14}$	1454	0.0001	0.3
100	10	$8.33\cdot10^{-13}$	1454	0.001	0.3
100	100	$8.33\cdot10^{-12}$	1454	0.01	0.3

[1] T_{min} refers to the shortest arrival time for seepage water as defined in equation (8).

$$\Theta = \left[1 + \left(\psi/\psi_o\right)^n\right]^{-m} \tag{4}$$

$$k_r = \sqrt{\Theta}\left[1 - \left(1 - \Theta^{1/m}\right)^m\right]^2 \tag{5}$$

where $\Theta = (\theta - \theta_s)/(\theta_s - \theta_r)$ is water saturation (with θ = volumetric water content, θ_s = water content at saturation, and θ_r = residual water content), ψ [M L^{-1} T^{-2}] is capillary pressure, and n and m=1–1/n are model parameters. Hydrologic properties of fracture continuum calculated using Equations (1)–(3) are shown in Table 1, for four different fracture apertures at three different densities.

A 1D column model representing the fracture continuum was developed using multiphase flow and transport simulator iTOUGH2 [8]. The model has a cross-sectional area of 1 m^2 and is sliced into 800 1 cm thick grid cells (representing the 8 m thick column of fractured rock between the +10 level and the adit ceiling).

Constant net precipitation (precipitation in excess of evaporation losses) flux is applied to a top boundary element for the duration of the rain event. In this paper, we report the results of 6 hr rain events only. We considered rainfall events of three net precipitation intensities – 0.5 mm/hr, 1 mm/hr, and 2 mm/hr – resulting in total net precipitation (hence, infiltration) volumes of 3, 6, and 12 L per event for the model cross-sectional area.

The precipitation water infiltrates into the fractured tuff at a rate determined by the fracture properties. Excess precipitation not taken by the fractured tuff immediately is allowed to pond at the surface and infiltrates into the tuff gradually. Considering that the +10 level is nearly horizontal, runoff generation is ignored, and evaporative loss is not incorporated into this model. Because dripping water has a slightly positive internal pressure, the percolating water seeps into the adit only after the saturation at the adit ceiling has reached unity (zero capillary pressure).

In this paper, we report simulation results for fracture apertures of 10 and 100 μm at a fracture density of 10 m^{-1}. Note that the permeability of the 100 μm fracture continuum is three orders of magnitude higher than that of the 10 μm continuum (see Equation (1) and **Table 1**). The corresponding hydrologic parameters were taken from **Table 1**. The *van Genuchten* parameter $1 < n < \infty$, which is a measure of the aperture size distribution, was assumed to be 5.

II.B. Model Results

The infiltration rate at +10 level and the corresponding seepage rate at the adit for the columns with mean fracture aperture of 10 and 100 μm are given in **Figures 2 and 3**, respectively.

The saturated hydraulic conductivity of the 10 μm column is lower than all of the precipitation fluxes. Hence, the infiltration rate is consistently higher than the hydraulic conductivity. Initially, the infiltration rate starts with a very high value because of the additional strong capillary pressure gradient at the wetting front. The infiltration rate asymptotically approaches the saturated hydraulic conductivity. Although the duration of the precipitation is only 6 hrs, ponded infiltration is predicted to persist for 1 to 3 days. Note that the evaporation from such ponded conditions is not considered. For the 0.5 mm/hr precipitation scenario, the wetting front arrives at the adit several minutes after infiltration has stopped. This differs from the 1 mm/hr and 2 mm/hr scenarios, where seepage starts well before infiltration has stopped. For the situation where infiltration and seepage occur simultaneously, the fracture continuum remains fully saturated. During this time, the seepage rate reaches its maximum value, which is equal to the saturated hydraulic conductivity.

In contrast, the saturated hydraulic conductivity of

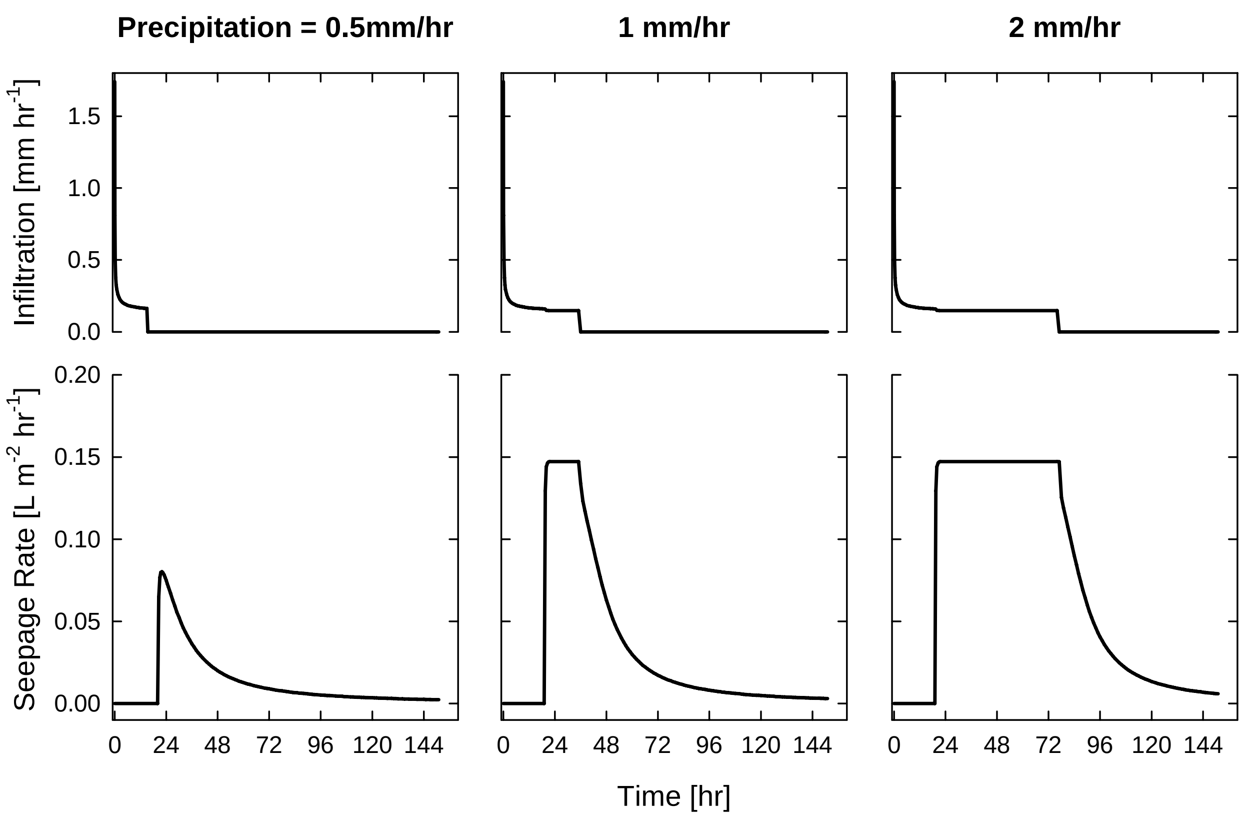

Figure 2. Infiltration rate and seepage rate for a 1D column of fracture continuum with mean fracture aperture of 10 μm and fracture density of 10 m^{-1}. The simulated net precipitation (supply of water) values are 0.5, 1, and 2 mm/hr for duration of 6 hrs.

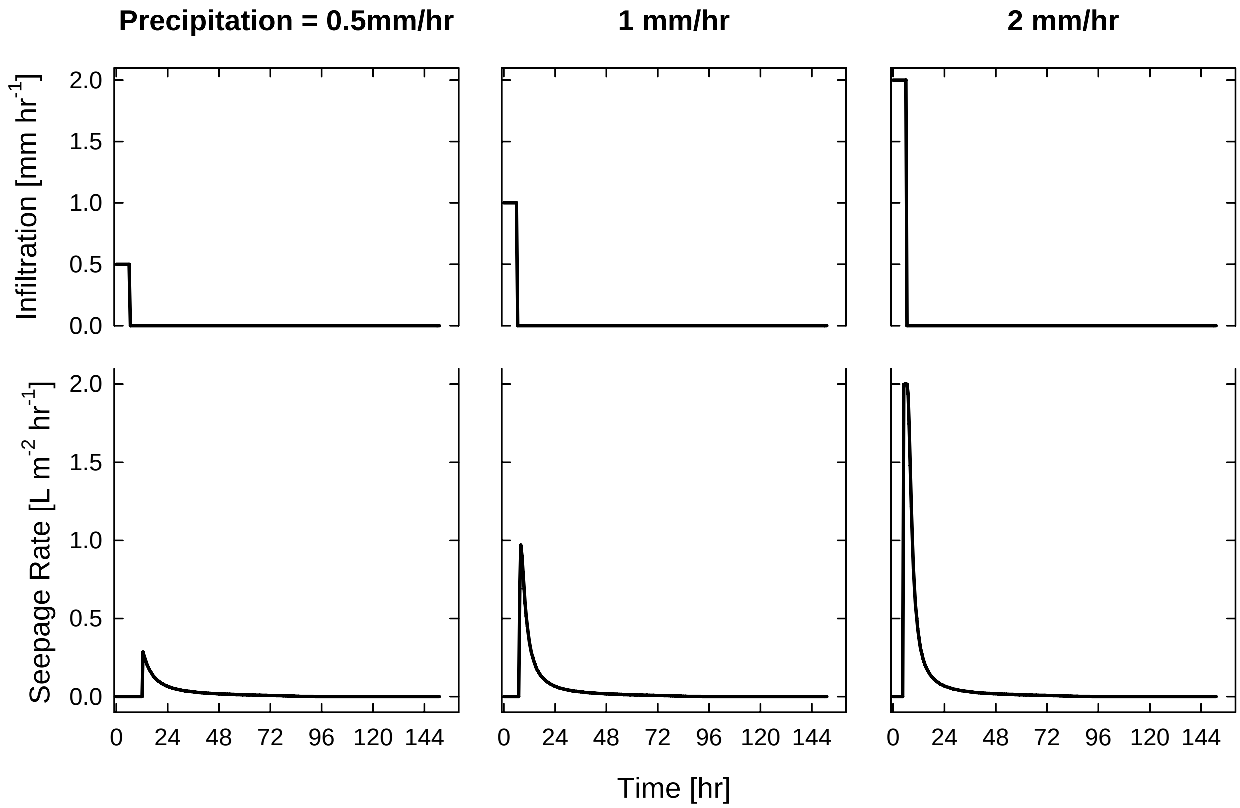

Figure 3. Infiltration rate and seepage rate for a 1D column of fracture continuum with mean fracture aperture of 100 μm and fracture density of 10 m^{-1}. The simulated net precipitation (supply of water) values are 0.5, 1, and 2 mm/hr for duration of 6 hrs.

the 100 μm column is higher than all the precipitation fluxes considered. Thus, the precipitation water is taken up by the fractured tuff as soon as it is deposited on the surface and the infiltration period coincides with the precipitation period of 6 hrs. For the three precipitation rates considered, the wetting front arrives at the adit in less than one day. The initial seepage rate of the 100 μm fracture column is much higher than for the 10 μm column because of the higher absolute permeability of the former. Nevertheless, the seepage rate is lower than the potential maximum (saturated hydraulic conductivity) because the column is not fully saturated everywhere, and the flow to the adit is less than its potential maximum.

The seepage rate is highest at the start of seepage and gradually decreases, because water held back just above the adit ceiling before seepage starts is released into the adit at a high rate after a positive pressure is achieved. Subsequent to that, the percolating water seeps as it arrives, as long as the seepage condition is met.

III. ANALYTICAL CONSTRAINTS

One of the goals of this preliminary assessment is to understand how the different features of fractures at

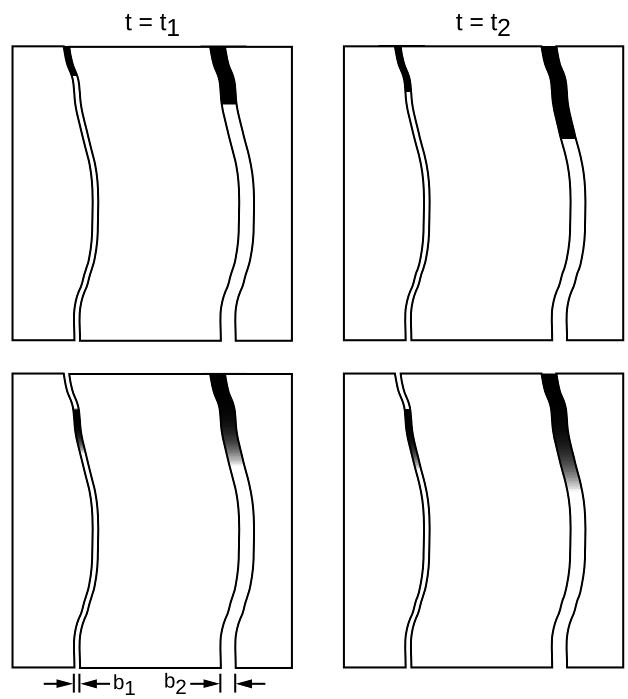

Figure 4. Flow of water plume along idealized fractures of different apertures. The top row shows intact plumes of 100% saturation, whereas the bottom row has diffused advancing and receding fronts.

Nopal I will affect the spatial and temporal distribution of seepage. In this section, we derive analytical constraints for the arrival of seepage water at the adit.

The basic assumption for developing the analytical constraints is that the plume of percolating water travels as an intact body of water of uniform saturation as illustrated in **Figure 4** (top row). In reality, because of capillary pressure gradients at the leading and trailing edges of the plume, the front and back edges, respectively, have diffused saturation profiles as illustrated in **Figure 4** (bottom row).

The velocity of the plume v [L T^{-1}] is related to the hydraulic conductivity K [L T^{-1}] and the porosity of the fractures as

$$v = K/\phi \qquad (6)$$

The hydraulic conductivity depends on the magnitude of the precipitation rate i [L T^{-1}] relative to the saturated hydraulic conductivity K_S. Specifically, if the infiltration rate is less than the K_S, then the unsaturated hydraulic conductivity is equivalent to the precipitation rate. Mathematically, this can be written as

$$\begin{aligned} K &= K_S \quad \text{if } i \geq K_S \\ K &= i \quad \text{otherwise} \end{aligned} \qquad (7)$$

where $K_S = \rho g\, k/\mu$, ρ [M L^{-3}] is the water density, g [L T^{-1}] gravitational acceleration, and μ [M L^{-1} T^{-1}] is viscosity of water.

Then, the time it takes for the leading edge of the water plume to arrive at the adit is simply given as

$$T = D/K \qquad (8)$$

where D [= 8 m] is the vertical distance between the +10 level and the adit ceiling. Estimates of shortest arrival times for different fracture apertures and fracture densities are given in **Table 1**.

In **Figure 5**, calculated arrival time (in hours) are shown as a function of precipitation rate for different values of fracture aperture and fracture density. If the fractures are unsaturated, the arrival time decreases as the precipitation rate increases. The shortest arrival time (fully saturated fractures) is determined by the plume velocity given in equation (6). In **Figure 5a**, the fracture density is fixed at 10^{-1} m and four different values of fracture aperture are considered. The shortest arrival time decreases as fracture aperture increases. This trend is explained by noting that according to equations (1), (3), and (6), the maximum plume velocity (inverse of the shortest arrival time) is related to the fracture aperture as $v \sim b^2$. In contrast, the shortest arrival time does not change with changes in fracture density (**Figure 5b**) for a fracture aperture of 20 μm. Note that the plume velocity is not dependent on fracture density.

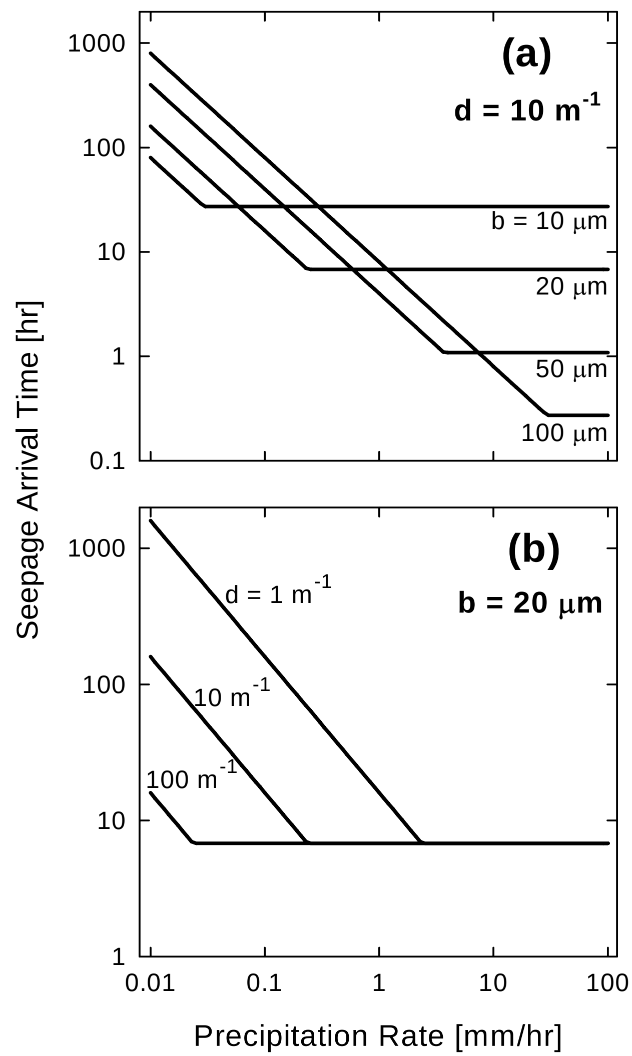

Figure 5. Arrival time of seepage water as a function of precipitation rate for (a) fracture density of 10 m^{-1} and (b) fracture aperture of 20 μm.

IV. SUMMARY

The results reported in this paper provide insights into how the fracture aperture and fracture density determine arrival time of seepage water and pattern of seepage flux. The highest seepage rate is equivalent to the saturated hydraulic conductivity of the fractures (which occurs only if the fracture column is saturated at high precipitation rates). When seepage occurs at this maximum rate, it also remains at constant rate for the time that the column is fully saturated (infiltration and seepage also occur simultaneously). If such observations are made in the field, they can be used to estimate the local saturated hydraulic conductivity of the formation.

Certain limitations in the results presented within this paper, which will be addressed as more information becomes available, include:

1. The cross-section of the column is uniformly restricted to 1 m^2 and all fractures are assumed perfectly vertical. These limitations can be improved by considering a tortuosity factor and/or multiple interacting columns.

2. The 1D model presented here considers only vertical continuous fractures. Fracture discontinuities and dip will increase the flow path and decrease the gradient, thereby reducing the arrival time substantially. Overestimation of permeability by the cubic-law (e.g., for fractures with sharp irregularities [5, 6]) also overpredicts the arrival time.

3. Given that fractures sets of different apertures and densities (permeability regimes) may occur adjacent to each other, precipitation water ponded over low permeabilities regions may be diverted to high permeability areas.

4. Matrix seepage and storage have not been considered in these analyses.

ACKNOWLEDGMENTS

This work is supported by the Director, Office of Civilian Radioactive Waste Management, Office of Science and Technology and International, of the U.S. Department of Energy under Contract No. DE-AC02-05CH11231. We would like to thank Alba Luz Saucedo for her assistance in the field as well as Yingqi Zhang and Dan Hawkes for their constructive reviews

REFERENCES

[1] Green, R.T. and G. Rice. *Numerical analysis of a proposed percolation experiment at the Peña Blanca natural analog site*. in *Sixth Annual International Conference on High Level Radioactive Waste Management*. 1995. Las Vegas, Nevada: ASCE. 226-228.

[2] Pearcy, E.C., J.D. Prikryl, and B.W. Leslie, Uranium transport through fractured silicic tuff and relative retention in areas with distinct fracture characteristics. Applied Geochemistry 1995; 10: 685-704.

[3] Witherspoon, P.A., J.S.Y. Wang, K. Iwai, and J.E. Gale, Validity of Cubic Law for Fluid-Flow in a Deformable Rock Fracture. Water Resources Research 1980; 16: 1016-1024.

[4] Witherspoon, P.A., C.H. Amick, J.E. Gale, and K. Iwai, Observations of a Potential Size Effect in Experimental-Determination of the Hydraulic-Properties of Fractures. Water Resources Research 1979; 15: 1142-1146.

[5] Dijk, P.E. and B. Berkowitz, Three-dimensional flow measurements in rock fractures. Water Resources Research 1999: 3955-3959.

[6] Oron, A.P. and B. Berkowitz, Flow in rock fractures: The local cubic law assumption reexamined. Water Resources Research: 2811-2825.

[7] van Genuchten, M.T., A Closed-Form Equation for Predicting the Hydraulic Conductivity of Unsaturated Soils. Soil Science Society of America Journal 1980; 44: 892-898.

[8] Finsterle, S., iTOUGH2 User 's Guide. 1999, Lawrence Berkeley National Laboratory: Berkeley.